Highlights

An equivalent plate model for assessing the dynamic behavior of highly damped sandwich plates

Rafael da S. Raqueti, Noureddine Atalla, Morvan Ouisse, Emeline Sadoulet-Reboul

- Highly damped sandwich plates are modeled using an equivalent plate representation
- Damping is determined via power balance and a wave approach for the forced response
- The proposed model is suitable for describing highly damped sandwich plates
- Computational time for estimating the behavior on a large frequency band is reduced

An equivalent plate model for assessing the dynamic behavior of highly damped sandwich plates

Rafael da S. Raqueti[a,b], Noureddine Atalla[a], Morvan Ouisse[b], Emeline Sadoulet-Reboul[c]

[a] *Université de Sherbrooke, Centre de recherche acoustique-signal-humain (CRASH-UdeS), 2500 boul. de l'Unviersité, Sherbrooke (Québec), J1K 2R1, Canada*
[b] *SUPMICROTECH, Université de Franche-Comté, CNRS, Institut FEMTO-ST, F-25000 Besançon, France*
[c] *Université de Franche-Comté, CNRS, Institut FEMTO-ST, F-25000 Besançon, France*

Abstract

This article presents an equivalent plate modeling approach for assessing the dynamic behavior of highly damped multilayered plates, with a focus on adaptive structures with shape memory polymer core. The mechanical properties of these structures vary with frequency and temperature, and exceptional damping values are obtained near the glass transition temperature of the shape memory polymer. By modeling the system as an equivalent homogeneous and isotropic thin plate, the effective properties are analytically determined by retaining the real parts of the bending, shear (transverse) and extension (quasi-longitudinal) waves. Unlike other equivalent plate models, the damping loss factor is estimated using a power balance formulation accounting for the significance of multiple waves types, improving the description of the dissipation mechanism. The results show good agreement with the damping estimates obtained using the power input method and the full order finite element model of the sandwich plate. For a 4% damping value, the equivalent plate finite element model accurately predicts the vibroacoustic indicators of the adaptive sandwich plate, while significantly reducing the modeling complexity. Even at exceptionally high damping levels (55% and 77%), the equivalent plate model captures the overall dynamic behavior of the structure. This proposed equivalent model offers a practical method for evaluating the vibroacoustic performance of highly damped multilayered plates and can be used to explore various behaviors of adaptive sandwich plates. Its reduced computation time makes it especially suitable for optimization problems, such as determining optimal temperatures for damping and stiffness control.

Keywords: equivalent plate modeling, adaptive sandwich plates, shape memory polymer, damping estimation, vibration control

1. Introduction

The energy, aerospace, and transportation industries are developing complex mechanical systems composed of multilayered composite materials. These materials are characterized by a high specific modulus, achieving desirable mechanical properties, *e.g.* stiffness, with reduced total mass. However, reinforcement materials typically exhibit low damping capacity, making the enhancement of the dynamical behavior of multilayered structures an ongoing research challenge. One approach to reduce vibrations is to constrain viscoelastic materials within the multilayered structure [1]. By doing so, energy is dissipated through shear motion mechanisms, increasing the structural damping. This passive solution is simple to implement and particularly effective to attenuate high-frequency vibrations. However, some applications may require a significant thickness of the viscoelastic layers, which increases the total mass of the structure. Additionally, this solution lacks adaptability, as the thickness of the viscoelastic layers cannot be adjusted.

In recent years, multilayered composite structures have achieved better performance by incorporating smart materials, such as Shape Memory Polymers (SMPs) [2]. An example is the tBA/PEGDMA, whose constitutive equation was characterized by Butaud *et al.* [3]. Its mechanical properties (storage and loss moduli) are frequency and temperature-dependent, enabling the development of solutions for noise and vibration control with adjustable properties. For instance, Butaud *et al.* [4] presented an adaptive sandwich plate where vibration levels can be reduced by adjusting the core's temperature. Similarly, Ouisse *et al.* [5] increased the damping and improved the acoustic black hole effect through temperature adjustments. In another study, Butaud *et al.* [6] presented an airplane model with sandwich wings achieving concurrent control of damping and stiffness. Although internal temperature adjustment poses challenges for implementation and monitoring, these examples demonstrate interesting performance across a wide range of applications when compared to commonly adopted solutions due to the adaptability.

In references [4, 6], adaptive sandwich structures were modeled using high-fidelity finite element models, specifically with 3D solid elements. These models demonstrated a good agreement with experimental data [4, 6]. Additionally, this modeling approach effectively accounts for thermal gradients effects caused by temperature differences between patches and along the transverse direction in the SMP core [6]. However, employing these models in optimization strategies, such as the one adopted by Butaud *et al.* [6], becomes impractical for systems with a large number of degrees of freedom due to their high computational cost. Model order reduction techniques, like those discussed by Rade *et al.* [7], can alleviate computational cost, but they require extensive mathematical tools.

Alternative modeling strategies involve using simplified physical descriptions: 1) adopting kinematic and stress simplifications on the layers of the structure; 2) multilayered structures are approximated as equivalent plates. These approaches reduce the number of degrees of freedoms compared to full order models, resulting in less computational time at the cost of accuracy. Depending on the application, the loss of accuracy may be accepted, and these models can be used as a numerical tool to understand the dynamic behavior of multilayered plates in the early design stages. Moreover, with appropriate accuracy levels, these approaches can even be used to solve optimization problems, such as determining thermal configurations for the balance between vibrations reduction and stiffness [6].

Modeling the multilayered structure using the finite element method remains convenient due to its well-established theoretical background, and ability to handle various boundary conditions. In particular, certain assumptions about displacement fields can be applied, as in the Equivalent Single Layer, Layer-Wise (LW) and Zig-Zag theories [8, 9]. Their performance depends on the ability to accurately describe bending, shear and other kinematic mechanisms within the structure. Among these ones, the General Laminate Model (GLM) [10] is a LW model in which the displacement fields account for transverse shear deformation and other kinematic mechanisms. The GLM is used in this work to estimate the dispersion relations for the sandwich plate. Alternatively, the Wave Finite Element (WFE) [11, 12] can be used. In these cases, although the response depends on the properties of the layers, damping is treated separately and incorporated as a structural parameter [10, 11, 12]. Alternatively, the Highly Contrasted Stratified (HCS) plate model [13, 14] describes the dynamical behavior of HCS plates with strongly contrasting layers by incorporating specific kinematic descriptors and using an asymptotic approach. Like the GLM, the HCS plate model does not take into account variations in mechanical properties along the core of the sandwich plate.

Among all these techniques, equivalent plate models have gained particular attention in the vibroacoustics community over the years. Indeed, these methods are able to provide mechanical properties that can be included in numerical models of large size to estimate quantities of interest in structural dynamics that mainly involve transverse displacements, such as quadratic velocity or acoustic radiation. One of the most popular approaches was developed by Ross, Kerwin and Ungar (RKU model) [15]. This model describes sandwich plates with viscoelastic core (frequency and temperature-dependent materials) by estimating a complex flexural rigidity. However, it is limited to three-layers structures. Guyader's method [16, 17] can be seen as an alternative and more general, as it provides the frequency-dependent equivalent bending rigidity of multilayered panels. Arasan *et al.* [18] simplified Guyader's model based on the asymptotic behavior of the natural propagating wavenumber for sandwich panels, allowing the bending stiffness to be determined using a sigmoid function [18]. Ege *et al.* [19] compared the RKU and Guyader's models for sandwich plates with different core stiffness. Their studies revealed differences in the equivalent damping loss factor, despite both models adopting the same damping definition [19].

Analytically, different approaches exist to determine the structural damping [20]: a wave domain definition (that can be simplified in the case of thin plates under bending); and an energetic definition [11, 12, 10]. However, these models use simplified damping definition in their formulation and are not validated for highly damped multilayered plates. More recently, Cui *et al.* [21] used a wave approach to estimate damping by combining the power balance equation, demonstrating numerically adequate damping estimates for sandwich plates with highly damped viscoelastic core. Using the same wave approach with the GLM formulation [10], Tuozzo and Atalla [22] developed a homogenization strategy for multilayered structures (plates and shells).

To the best of the authors' knowledge, the literature lacks equivalent plate models that adequately assess the behavior of highly damped multilayered structures. Most available models rely on simplified definitions of the damping loss factor, either through equivalent or energetic formulations. This article aims to present a methodology for calculating the effective properties of an equivalent single-layer plate, incorporating an improved damping estimate. This model enables the evaluation of the vibroacoustic indicators of highly damped multilayered plates. Moreover, it facilitates the exploration and understanding of the various behaviors of adaptive sandwich structures, making it suitable for solving optimization problems thanks to its significantly reduced computational complexity.

This document is structured as follows: Section 2 describes the methodology for calculating the effective properties of the equivalent plate representing highly damped multilayered plates, and details the estimation of the structural damping loss factor. Section 3 compares the responses of the equivalent plate finite element model and the sandwich plate full order finite element model under various temperature fields and boundary conditions. Finally, Section 4 presents the conclusions of this work.

2. Materials and methods

This study considers a rectangular sandwich plate with homogeneous and isotropic skins, and a viscoelastic core. A transverse harmonic point load $\overrightarrow{f}(\omega)$ with angular frequency ω can be applied at any location of the sandwich plate's domain. The boundaries are denoted B1-B2-B3-B4, and various boundary conditions can be assumed: Free (F), Simply Supported (SS) and Clamped (C), *e.g.*, C-F-F-F stands for a cantilever plate. The considered sandwich plate is symmetric, but the methodology can be applied to other stratified structures (sandwich or multilayered plates, symmetric or asymmetric configurations, etc.). Figure 1 shows the sandwich plate and its equivalent plate representation.

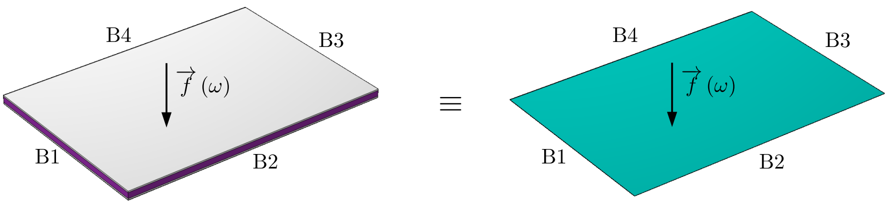

Figure 1: A sandwich plate with a homogeneous viscoelastic core is represented as an equivalent plate.

The viscoelastic core of the sandwich plate is in tBA/PEGDMA, which is a shape memory polymer whose mechanical properties are frequency and temperature dependent. The constitutive equation of the tBA/PEGDMA is characterized by Butaud *et al.* [3]. Equation 1 (2S2P1D model) describes its complex modulus E^*:

$$E^* = E_0 + \frac{E_\infty - E_0}{1 + \gamma(j\omega\tau)^{-k} + (j\omega\tau)^{-h} + (j\omega\beta\tau)^{-1}}, \tag{1}$$

where $j = \sqrt{-1}$ and $\omega = 2\pi f$. The parameter $\tau(T) = a_T(T)\tau_0$ depends on the temperature T and is defined by Equation 2 (WLF equation). Other parameters used in Equations 1 and 2 are given in Table 1.

$$\log(a_T) = \frac{-C_1^0(T - T_0)}{-C_2^0 + T - T_0}. \tag{2}$$

E_0 (Pa)	E_∞ (Pa)	γ	β	k	h	C_1^0	C_2^0 (K)
0.67	2,221	1.68	38,000	0.16	0.79	10.87	32.57

Table 1: Parameters used in Equations 1 and 2. T_0 = 313.15 K and τ_0 = 0.61 s.

The complex modulus E^* can be formulated in terms of the storage modulus E' and loss factor $\tan(\delta)$, as formulated in Equation 3:

$$E^* = E'(1 + j\tan(\delta)), \quad E' = \Re(E^*) \quad \text{and} \quad \tan(\delta) = \frac{\Im(E^*)}{\Re(E^*)}, \tag{3}$$

where $\Re(E^*)$ represents the real part and $\Im(E^*)$ the imaginary part of E^*. Figure 2 shows the storage modulus and loss factor of the tBA/PEGDMA for the frequency range from 10 Hz to 5,000 Hz, and temperatures between 20°C and 120°C:

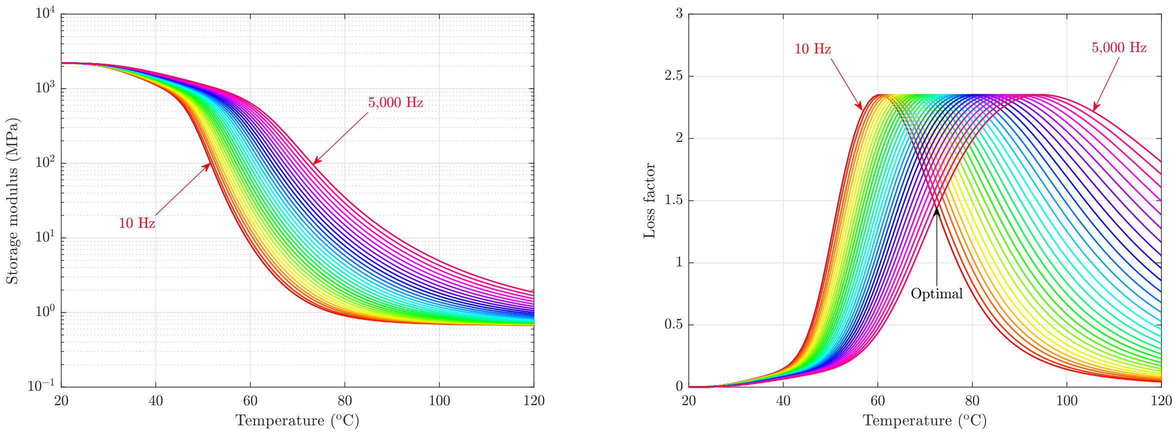

Figure 2: Storage modulus and loss factor of the tBA/PEGDMA: the optimal temperature defines a high loss factor value to reduce vibrations in the whole frequency range [4].

In Figure 2, the loss factor significantly increases close to the polymer's glass transition temperature, and it is possible to select an optimal temperature for which the loss factor is high in the whole considered frequency range [4]. Vibrations can be significantly reduced at this temperature, considering that the loss factor is extremely high compared to standard materials. However, at high temperatures, there is an inherent reduction of the storage modulus, affecting the structural stiffness of the sandwich plate. There is no advantage in increasing the temperature over 83°C because there is a damping decrease.

To reduce vibrations while maintaining structural stiffness, the sandwich plate can be divided into regular patches [6, 23]. A spatial "degradation" strategy can be applied by heating certain patches to increase damping, while keeping others at low temperature to preserve high stiffness levels. By doing so, a compromise between damping and stiffness can be achieved by combining various homogeneous temperature fields along the tBA/PEGDMA core. This type of configuration will be used as an illustrative example in the results section of this paper.

2.1. *Effective properties calculation*

It is assumed that the sandwich plate is represented as an equivalent thin plate. The finite element implementation of the governing equation of motion for the equivalent plate is given in Equation 4:

$$\left([\tilde{\mathbf{K}}^*] - \omega^2[\tilde{\mathbf{M}}]\right)\left\{\hat{\mathbf{U}}\right\} = \left\{\hat{\mathbf{F}}\right\}, \tag{4}$$

where $\left\{\hat{\mathbf{U}}\right\}$ is a vector containing rotations and transversal displacements, and $\left\{\hat{\mathbf{F}}\right\}$ is a vector containing the external forces. The mass matrix $[\tilde{\mathbf{M}}]$ and the complex stiffness matrix $[\tilde{\mathbf{K}}^*]$, which includes damping effects, are determined in function of the parameters of the equivalent plate. The effective properties are calculated by preserving the real parts of the bending k_B, shear (transverse) k_T and extensional (quasi-longitudinal) k_L wavenumbers of the original structure. Equations 5, 6 and 7 express these wavenumbers in terms of the physical and mechanical properties of an equivalent homogeneous and isotropic thin plate:

$$k_B^4 = \frac{12\tilde{\rho}\left(1 - \tilde{\nu}^2\right)}{\tilde{E}\tilde{h}^2}\omega^2, \tag{5}$$

$$k_T^2 = \frac{2\tilde{\rho}\left(1 + \tilde{\nu}\right)}{\tilde{E}}\omega^2, \tag{6}$$

$$k_L^2 = \frac{\tilde{\rho}\left(1-\tilde{\nu}^2\right)}{\tilde{E}}\omega^2. \tag{7}$$

The effective properties are formulated by rearranging Equations 5, 6 and 7, with their explicit formulas provided in Table 2. The mass of the sandwich plate is conserved, and the effective density $\tilde{\rho}$ is calculated by dividing the area density ρ_S over the effective thickness $\tilde{h}$. Equation 8 is the effective bending stiffness $\tilde{D}$ of the equivalent plate, where $\tilde{E}$ is the effective Young's modulus and $\tilde{\nu}$ the effective Poisson's ratio. These properties depend on both frequency and temperature.

Thickness (m)	Density (kg/m^3)	Poisson's ratio	Young's modulus (Pa)
$\tilde{h} = \sqrt{12}\frac{k_L}{k_B^2}$	$\tilde{\rho} = \frac{\rho_S}{\tilde{h}}$	$\tilde{\nu} = 1 - 2\left(\frac{k_L}{k_T}\right)^2$	$\tilde{E} = \frac{12\tilde{\rho}\left(1-\tilde{\nu}^2\right)}{\tilde{h}^2 k_B^4}\omega^2$

Table 2: Effective properties of the equivalent homogeneous and isotropic thin plate.

$$\tilde{D} = \frac{\tilde{E}\tilde{h}^3}{12\left(1-\tilde{\nu}^2\right)} \tag{8}$$

There are different methods to compute the wavenumbers of a sandwich plate: analytical [10], Wave Finite Element (WFE) [11, 12]. In this work, k_B, k_T and k_L are determined with the General Laminate Model (GLM) [10], that is described in Section 2.2.

Although the wavenumbers are complex quantities, with the imaginary part representing wave attenuation through the structure, this work only uses their real parts to calculate the effective properties in Table 2 and the effective bending stiffness in Equation 8. Dissipation mechanisms are incorporated into the system through a structural damping loss factor η, with the complex effective bending stiffness expressed as $\tilde{D}^* = \tilde{D}(1 + j\eta)$. Section 2.4 outlines various formulations for estimating the damping loss factor.

2.2. The General Laminate Model (GLM)

The bending, shear (transverse) and extension (quasi-longitudinal) wavenumbers can be determined using the General Laminate Model (GLM) [10]. The GLM is an analytical discrete model for multilayered plates containing an arbitrary number of layers (sandwich construction, symmetric or asymmetric configurations, etc.). The layers can be made of isotropic or orthotropic materials, neglecting or assuming damping. Viscoelastic materials with frequency-dependent mechanical properties can also be taken into account. In each layer, the displacement field is described by the First order Shear Deformation Theory (FSDT). Bending, in-plane and transverse shear, rotational inertia and interlayer forces are considered in the governing equations [10]. Symmetric and asymmetric modes are captured, including dilatational modes, through a complementary displacement field [10]. Assuming a harmonic solution, the dispersion relations are described by Equation 9:

$$\left(k^2(\omega,\varphi)\left[\mathbf{A}_2(\varphi)\right] - jk(\omega,\varphi)\left[\mathbf{A}_1(\varphi)\right] - \left[\mathbf{A}_{01}(\varphi)\right] - \omega^2\left[\mathbf{A}_{02}(\varphi)\right]\right)\{\mathbf{e}\} = 0, \tag{9}$$

where $\{\mathbf{e}\}$ is a mixed displacement-force vector (containing rotations, transversal displacement and interlayer forces) of size $5N + 3(N-1)$, with N the number of layers of the laminate.

For a given wave heading angle φ and in the presence of damping, $[\mathbf{A}_2]$, $[\mathbf{A}_1]$ (non-symmetric) and $[\mathbf{A}_{01}]$ are complex valued square matrices, resulting in $5N + 3(N-1)$ complex eigenvalues $k(\omega,\varphi)$. As Ghinet and Atalla [10] discussed, accounting for damping makes the sorting of the wavenumber difficult. An algorithm is defined to select propagating waves, where the imaginary part is less significant than the real part. Two additional conditions are applied: the continuity of the phase velocity and the maximum correlation between eigenvectors [24, 25]. Following this algorithm, the waves are sorted by their magnitude, such that $\|k_B\| > \|k_T\| > \|k_L\|$.

The GLM is designed for infinitely extended homogeneous multilayered plates and does not account for spatial variations in properties along the x and y-directions.

2.3. Wave-domain approach for the forced response

In this section, a wave-domain approach is described to compute some vibroacoustic indicators of multilayered plates. The GLM formulation presented in Equation 9 can be adapted to compute the forced response [26]:

$$\left(k^2(\omega,\varphi)[\mathbf{A}_2(\varphi)] - jk(\omega,\varphi)[\mathbf{A}_1(\varphi)] - [\mathbf{A}_{01}(\varphi)] - \omega^2[\mathbf{A}_{02}(\varphi)]\right)\{\mathbf{e}\} = \{\mathbf{f}\}, \tag{10}$$

where $k = \sqrt{k_x^2 + k_y^2}$ is the wavenumber, with $k_x = k\cos(\varphi)$ as the component along the x-axis and $k_y = k\sin(\varphi)$ as the component along the y-axis. A transverse point load vector $\{\mathbf{f}\} = \{\mathbf{F}\}\,\delta x\,\delta y$ is assumed, where δ represents the Dirac delta function, and $\{\mathbf{F}\}$ is a vector containing a scalar unit value applied to a transversal displacement degree of freedom, with zeros in all other components. The spatial Fourier transform of $\{\mathbf{f}\}$ is expressed as $\{\hat{\mathbf{f}}\} = \{\mathbf{F}\}$, and the wavenumber representation of the forced vibration response $\{\hat{\mathbf{e}}(k,\varphi)\}$ is obtained by solving:

$$\{\hat{\mathbf{e}}(k,\varphi)\} = \left(k^2(\omega,\varphi)[\mathbf{A}_2(\varphi)] - jk(\omega,\varphi)[\mathbf{A}_1(\varphi)] - [\mathbf{A}_{01}(\varphi)] - \omega^2[\mathbf{A}_{02}(\varphi)]\right)^{-1}\{\mathbf{F}\}. \tag{11}$$

The spatial domain representation of the forced vibration response $\{\mathbf{e}(x,y)\}$ can be determined using the inverse Fourier transform:

$$\{\mathbf{e}(x,y)\} = \frac{1}{4\pi^2}\int_{-\infty}^{\infty}\int_{-\infty}^{\infty}\left\{\hat{\mathbf{e}}\left(k_x,k_y\right)\right\}e^{-j\left(k_x x + k_y y\right)}\,dk_x\,dk_y. \tag{12}$$

For numerical efficiency, the double integral in Equation 12 is computed in a polar coordinate system. Since the GLM assumes infinite extent plates, the choice of (x,y) coordinates is arbitrary and, assuming the origin point $(x_0,y_0) = (0,0)$, $\{\mathbf{e}(0,0)\}$ is given by:

$$\{\mathbf{e}(0,0)\} = \frac{1}{4\pi^2}\int_0^{2\pi}\int_0^{\infty}\{\hat{\mathbf{e}}(k,\varphi)\}\,k\,dk\,d\varphi, \tag{13}$$

where $\{\hat{\mathbf{e}}(k,\varphi)\}$ is computed using Equation 11.

The same strategy can be used to compute other indicators, such as the dissipated power Π_d, kinetic energy E_c and strain energy E_d:

$$\hat{\Pi}_d(k,\varphi) = \frac{1}{2}\Im\left(\omega\,\{\hat{\mathbf{e}}(k,\varphi)\}^H[\mathbf{K}(\varphi)]\{\hat{\mathbf{e}}(k,\varphi)\}\right), \tag{14}$$

$$\hat{E}_c(k,\varphi) = \frac{1}{4}\omega^2\{\hat{\mathbf{e}}(k,\varphi)\}^H[\mathbf{M}(\varphi)]\{\hat{\mathbf{e}}(k,\varphi)\}, \tag{15}$$

$$\hat{E}_d(k,\varphi) = \frac{1}{4}\Re\left(\{\hat{\mathbf{e}}(k,\varphi)\}^H[\mathbf{K}(\varphi)]\{\hat{\mathbf{e}}(k,\varphi)\}\right), \tag{16}$$

where $\{\dots\}^H$ is the conjugate transpose and the matrices are $[\mathbf{K}(\varphi)] = k^2(\omega,\varphi)[\mathbf{A}_2(\varphi)] - jk(\omega,\varphi)[\mathbf{A}_1(\varphi)] - [\mathbf{A}_{01}(\varphi)]$ and $[\mathbf{M}(\varphi)] = [\mathbf{A}_{02}(\varphi)]$. The above indicators will be used later to compute the global damping loss factor of the sandwich plate.

2.4. Damping loss factor estimates

There are different damping definitions in the literature [20]. Equation 17 is a wave domain definition:

$$\eta = -2\frac{C_g}{C_\phi}\frac{\Im(k)}{\Re(k)}, \tag{17}$$

where C_g is the group velocity and C_ϕ is the phase velocity:

$$C_g = \frac{\partial\omega}{\partial\Re(k)}, \quad C_\phi = \frac{\omega}{k}. \tag{18}$$

In Equation 17, the $\frac{C_g}{C_\phi}$ ratio is bounded by $1 \leq \frac{C_g}{C_\phi} \leq 2$, where the plate's core is under shearing for the inferior bound and bending for the superior bound. When the thin plate assumptions are respected and the structure is slightly damped, an equivalent definition of damping can be used and Equation 19 holds:

$$\eta = -4\frac{\Im(k_B)}{\Re(k_B)}. \tag{19}$$

Note that Equations 17 and 18 assume low damping, as the group velocity C_g is undefined for high damping cases and should be replaced by an energy velocity.

Alternatively, damping can be estimated using the energetic definition in Equation 20, where $\{\mathbf{e}_i\}$ is the considered wave mode shape. Equation 20 has been adopted in previous studies based on LW representations [10, 11, 12]. However, this definition only accounts for the main propagating wave and is computed for the wave with the highest wavenumber at a given frequency.

$$\eta_i = \frac{2\Im\left(\{\mathbf{e}_i\}^H [\mathbf{K}] \{\mathbf{e}_i\}\right)}{\Re(\{\mathbf{e}_i\}^H ([\mathbf{K}] + \omega^2 [\mathbf{M}]) \{\mathbf{e}_i\})}. \tag{20}$$

Recently, Cui *et al.* [21] predicted the damping of highly dissipative meta-structures using the WFE. In their work, the estimation of Damping Loss Factor (DLF) is based on the Power Input Method (PIM) [27], in which the vibroacoustic indicators are estimated using the wave-domain approach. The same approach is used here to estimate the DLF using Equation 21:

$$\eta = \frac{\Pi_d}{\omega(E_c + E_d)}, \tag{21}$$

where Π_d represents the dissipated power, E_c the total kinetic energy and E_d the total strain energy. These quantities are determined by solving the forced response of the sandwich plate as described in Section 2.3:

$$\Pi_d(\omega) = \frac{1}{4\pi^2} \int_0^{2\pi} \int_0^{\infty} \hat{\Pi}_d(k, \varphi)\, k\, dk\, d\varphi, \tag{22}$$

$$E_c(\omega) = \frac{1}{4\pi^2} \int_0^{2\pi} \int_0^{\infty} \hat{E}_c(k, \varphi)\, k\, dk\, d\varphi, \tag{23}$$

$$E_d(\omega) = \frac{1}{4\pi^2} \int_0^{2\pi} \int_0^{\infty} \hat{E}_d(k, \varphi)\, k\, dk\, d\varphi. \tag{24}$$

The last method described can be applied to orthotropic multilayered plates. In this context, it integrates the contribution of multiple wave types accounting for the head angle φ, whereas other estimations consider only the contribution of a single wave type [12, 28].

This method (Equation 21), selected in this work, will be compared with the single wave based methods (Equations 17 and 20).

3. Results and discussion

The materials properties and dimensions of the rectangular sandwich plate are given in Table 3. Various cases are studied by assuming different boundary conditions and temperature field configurations. In three of them, a core with homogeneous mechanical properties is considered. This is obtained by assuming a homogeneous temperature field in Equation 1. In the last one, a heterogeneous temperature field is assumed by combining patches at different temperatures, resulting in heterogeneous mechanical properties along the core of the sandwich plate.

Layer	Thickness (mm)	Material	Density (kg/m^3)	Poisson's ratio	Young's modulus (GPa)	Loss factor
Skins	0.5	Aluminum	2,700	0.33	70	0.001
Core	2.2	tBA/PEGDMA	990	0.37	Fig. 2	Fig. 2

Table 3: Material properties and dimensions of the adaptive sandwich plate (length L_x = 1 m and width L_y = 0.7 m).

In the first part, the effective properties are determined using the explicit formulations in Table 2. These properties are compared with those obtained from Guyader's model [16, 17]. Simultaneously, the structural damping loss factor is computed using the power balance equation and energy indicators from the GLM forced response formulation. The adequacy of this damping estimation method is assessed by comparing it with a reference estimation approach.

Subsequently, the effective properties are used to construct an equivalent single layer plate (2D) finite element (FE) model. The performance of the proposed equivalent plate FE model is analyzed through local and global vibroacoustic indicators. These responses are compared with those obtained from a high-fidelity finite element model, which uses 3D solid elements for both the skins and the core.

3.1. Estimation of the effective properties

Initially, three core's temperature are considered: 50°C, 65°C and 80°C.

- At 50°C, the tBA/PEGDMA exhibits a high storage modulus (approximately 1.04 GPa) and moderate damping (around 19%).
- At 65°C and 80°C, the storage modulus is significantly reduced (0.24 GPa and 0.02 GPa, respectively), while the loss factor is considerably higher (108% and 213%, respectively), across the entire frequency range. In these latter cases, the sandwich plate exhibits a soft core and is highly damped.

To illustrate the adaptability of the sandwich plate, the group and phase velocities of the main (bending) wave are estimated. The group velocity is determined numerically using a polynomial interpolation function of $k(\omega)$. Alternatively, it can also be computed explicitly using the GLM [22]. Figure 3 presents the evolution of the $\frac{C_g}{C_\phi}$ ratio for the studied temperatures. The sandwich plate exhibits different behaviors, transitioning from a bending-dominated to an increasingly shear-influenced response as the core temperature and frequency rises. While the group velocity is plotted for 80°C in Figure 3, its physical significance become unreliable under such high damping condition. In this case, the group velocity no longer equals the energy velocity, and an alternative definition based on energy velocity may be more appropriate [29]. However, this is not investigated further here since the power balance based definition (Equation 20) is more appropriate compared to the kinematic-based definition (Equation 17).

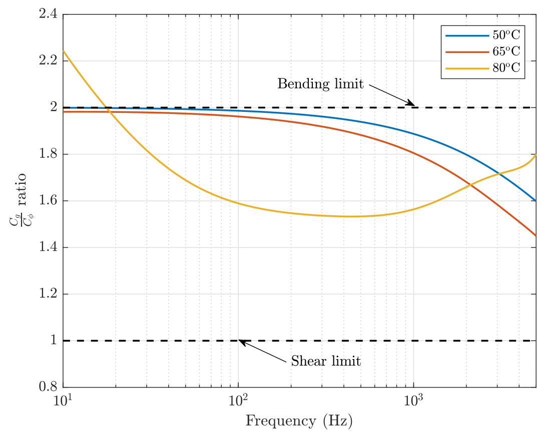

Figure 3: Evolution of the $\frac{C_g}{C_\phi}$ ratio at 50°C, 65°C and 80°C: the sandwich plate exhibits various behaviors in function of the core's temperature.

The assumption is that the proposed equivalent plate model can describe the various behaviors of the sandwich plate through an effective bending stiffness (depending on the bending, shear and extensional waves) and a suitable damping estimate.

Figures 4, 5 and 6 compare the equivalent bending stiffness and damping loss factor to reference models at 50°C, 65°C and 80°C, respectively. For each case:

- Dispersion relations (bending, shear and extensional wavenumbers) are determined using the GLM [10]. During these computations, the damping material properties are not neglected, but only the real parts of the wavenumbers are used to calculate the effective properties. The effective bending stiffness are compared to the ones computed with Guyader's model [17];

- Reference damping values of the sandwich plate are obtained numerically by simulating PIM tests, in which the indicators are computed with a high-fidelity finite element model (using 3D quadratic solid elements for the three layers). Three randomly selected excitation locations were used, and the kinetic, strain and dissipated energies are averaged over these locations. Equation 21 is used to compute the DLF and different damping estimates are compared.

Since high-fidelity finite element models are used for numerical validation, their construction is detailed here. In all cases, the reference model is constructed using TET10 solid elements and solved using a direct frequency response analysis. One element is assigned to each layer in the transverse direction, including the viscoelastic core. Increasing the number of elements through the thickness did not influence the accuracy of the vibroacoustic indicators. Convergence was assessed in all cases using both composite damping and mean square velocity as indicators. The suitability of solid elements for this type of modeling was demonstrated by Butaud *et al.* [4], where finite element simulations showed good agreement with experimental results.

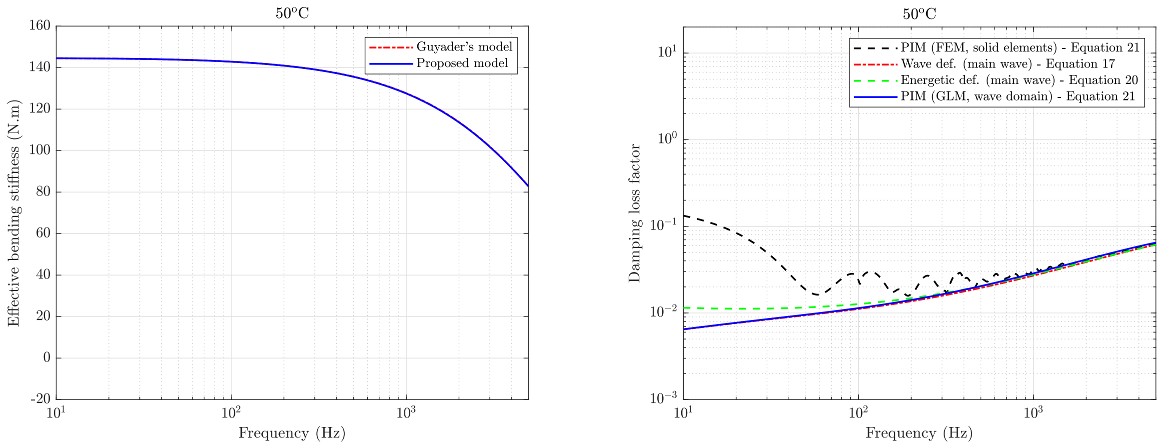

Figure 4: Effective bending stiffness and damping loss factor at 50°C (average DLF: 4%): the various damping estimates yield similar results.

At 50°C, the average damping across the entire frequency range is 4% (averaging the damping estimate from the power balance equation, using the GLM forced response). In this case, the analytical structural damping loss factor estimates show good agreement. At low and mid frequencies, discrepancies between these estimates and the reference damping - computed using Equation 21 and high-fidelity finite element models - are attributed to the finite dimensions of the structure, which introduce modal behavior. At higher frequencies, as the wavenumber increases, the modal effects diminish, and the sandwich plate behaves more like an infinite structure. In this case, the damping estimates align well with the reference. A similar modal behavior is observed at higher temperatures.

At 65°C and 80°C, the average damping across the entire frequency range is 55% and 77%, respectively. In these cases, both wave (Equation 17) and energetic (Equation 20) definitions fail to predict the DLF. In their formulation, these estimates consider the significance of a single wave (main wave). Instead, the PIM implementation in the wave-domain approach (Equation 21) accounts for the contribution of different waves types and its predictions of the DLF are in agreement with the reference finite element estimations. The effects of boundary condition become less significant as wavelengths decrease. This approach is feasible in terms of computational cost: damping can be estimated by solving a numerical integration rather than computing energy indicators using the high-fidelity finite element model of the sandwich structure.

As shown in Figures 5 and 6, the proposed methodology overestimates the effective bending stiffness compared to the Guyader's model. In the proposed approach, viscoelastic damping is considered in the calculation of the dispersion relations, influencing the magnitude of the wavenumbers. Additionally, the proposed model accounts for three main propagating waves, including shear and quasi-longitudinal motions. In contrast, Guyader's model considers only bending waves.

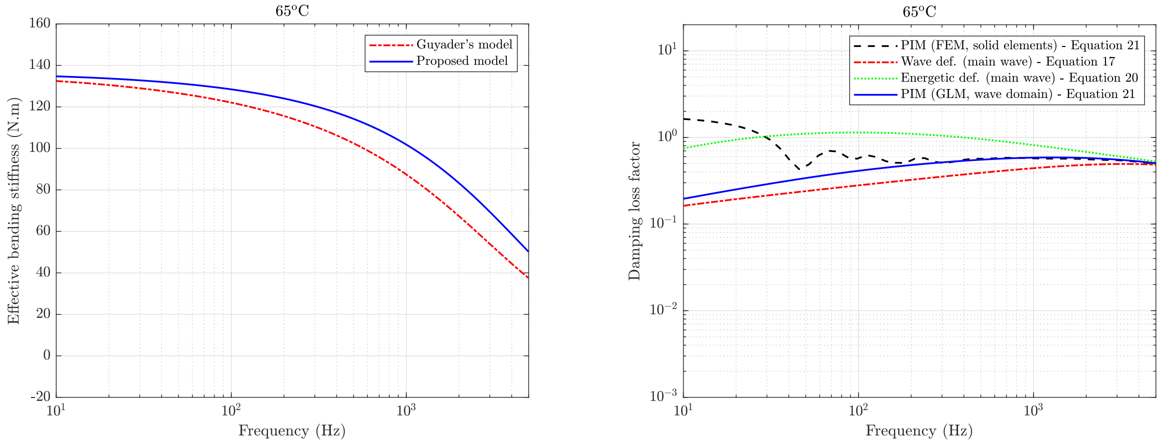

Figure 5: Effective bending stiffness and damping loss factor at 65°C (average DLF: 55%): damping estimates based only on the main wave fail to accurately describe the dissipation mechanisms. In contrast, the estimate based on the PIM, where the energy indicators are computed using the GLM, is accurate.

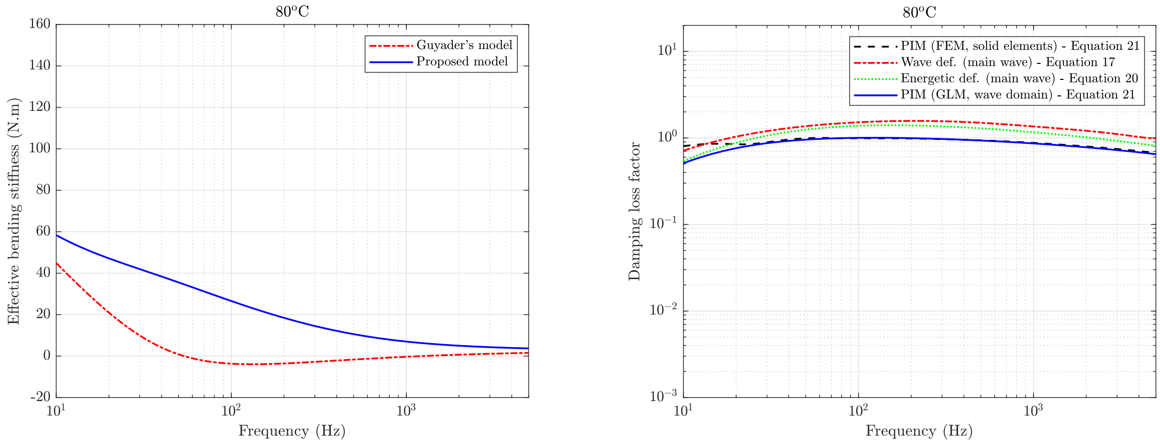

Figure 6: Effective bending stiffness and damping loss factor at 80°C (average DLF: 77%): the damping estimate based on the PIM accurately describes the dissipation mechanisms of the highly damped sandwich plate.

3.2. Responses of the proposed equivalent plate FE model

Using the effective properties (Table 2), the equivalent plate is defined using Discrete Kirchhoff Triangular Plate (DKTP) finite elements [30] and used to evaluate vibroacoustic indicators of the sandwich plate. GLM based wavenumbers (wherein complex valued properties are used but only the real parts of the wavenumbers are kept) and the PIM (wave-domain) damping estimate are used for determining the effective properties.

3.2.1. Homogeneous sandwich plate with a moderate damping level

Figure 7 shows the mean square velocity and the driving-point mobility of the sandwich plate with the core at 50°C. In this case, all edges of the structure are simply supported, and a unit centered point load is applied. There is a good agreement between the responses of the high-fidelity and the equivalent plate models. Note that both high-fidelity (TET10 solid elements in the three layers) and equivalent plate models (DKTP elements) were checked for convergence up to 5,000 Hz.

In Figure 7, the vibroacoustic indicators obtained using the analytical modal approach (Equation A.1) show good agreement with the reference indicators estimated using the high-fidelity model. In this case, the modal approach accurately represents the behavior of sandwich plate at 50°C across the entire frequency range.

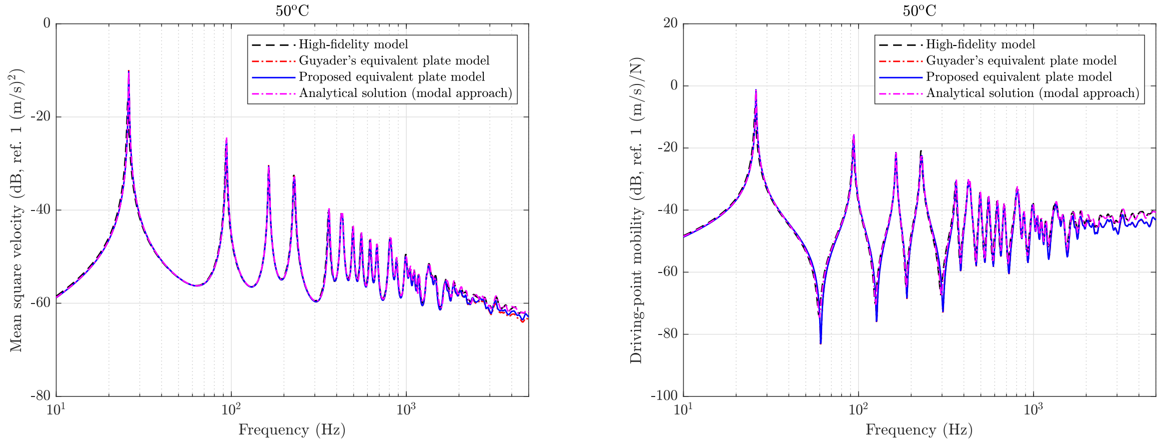

Figure 7: Mean square velocity and driving-point mobility of the simply supported (SS-SS-SS-SS) sandwich plate at 50°C: high-fidelity model (364,659 nodes); proposed equivalent plate model (2,337 nodes).

Both equivalent plate models exhibit similar trends, with the indicators closely matching up to 2,000 Hz. However, at higher frequencies, both models deviate in amplitude from the reference and modal approach solutions, underestimating the indicators. While the equivalent plate models define the effective properties by preserving a limited set of wavenumbers - bending, shear and quasi-longitudinal for the proposed model, and only bending for Guyader's model - the modal approach preserves modal impedance and does not rely on material assumptions, such as equivalent damping. At higher frequencies, additional modes become influential, contributing to the observed discrepancies.

Although not included in this paper for the sake of conciseness, the modal approach fails to accurately estimate the sandwich plate response when shear effects are significant (65°C and 80°C cases). In addition, this solution is limited to a few boundary conditions, and does not account for heterogeneous temperature fields.

3.2.2. Homogeneous sandwich plate with high damping levels

Figures 8 and 9 show the mean square velocity and the driving-point mobility of the sandwich plate at 65°C and 80°C, for various sets of boundary conditions. At 65°C, the structure is clamped, and at 80°C, the structure has two clamped and two simply supported edges. In both cases, a unit harmonic point load is applied at the center.

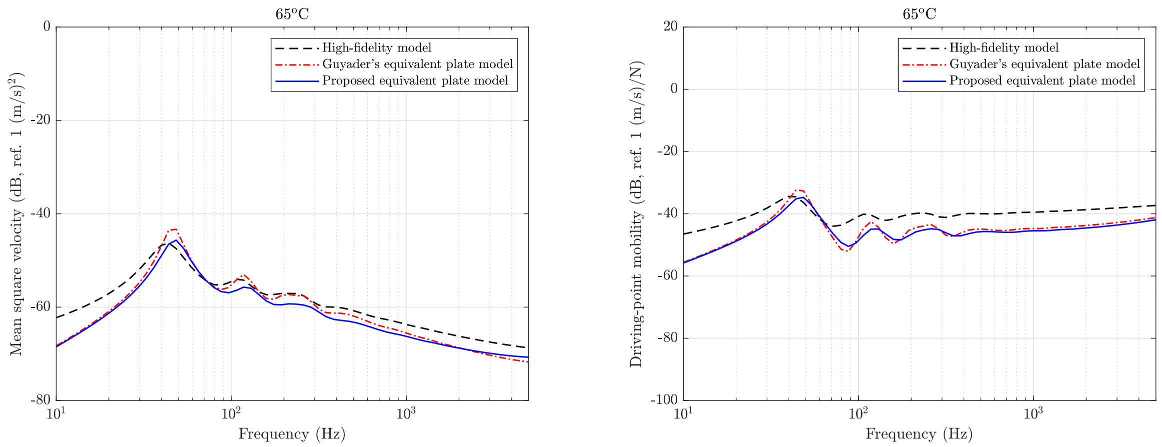

Figure 8: Mean square velocity and driving-point mobility of the clamped (C-C-C-C) sandwich plate at 65°C: high-fidelity model (471,308 nodes); proposed equivalent plate model (2,337 nodes).

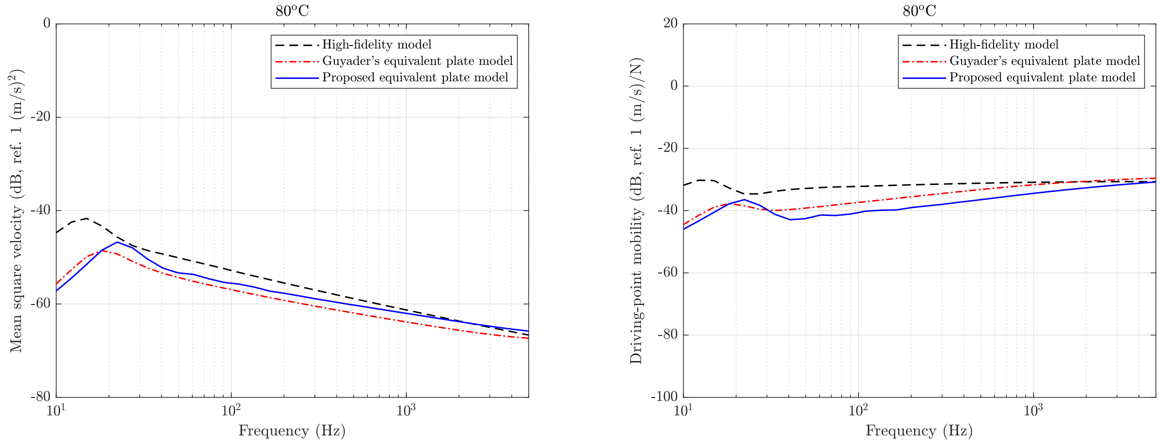

Figure 9: Mean square velocity and driving-point mobility of the sandwich plate with two clamped and two simply supported edges (C-C-SS-SS), at 80°C: high-fidelity model (825,687 nodes); proposed equivalent plate model (5,785 nodes).

At high temperature, the equivalent plate is systematically softer than the reference sandwich plate model, causing the "maxima" to shift to higher frequencies. This behavior is particularly noticeable in Figure 9. This may be caused by other deformation modes in the 3D FE model that the equivalent plate model does not fully represent.

Although the deviations of the vibroacoustic indicators are significant for both temperatures, the equivalent plate model is capable of qualitatively assessing the behavior of the structure. It is worth highlighting a significant reduction in the number of degrees of freedom required by the equivalent plate model. For the sandwich plate at 80°C case, the equivalent plate model estimates the vibroacoustic indicators in approximately one second per frequency step, whereas the high-fidelity model requires four minutes per frequency step on a workstation equipped with an Intel® Core™ i9-11950H processor (2.60 GHz) and 64 GB of RAM.

3.2.3. Heterogeneous sandwich plate with highly damped patches

Figure 10 shows an equivalent plate divided into sixteen regular patches, each assigned a different temperature. By allowing the temperature of each patch to be individually adjusted, the sandwich plate can be programmed to exhibit various behaviors. Compared to the previously analyzed homogeneous sandwich plates, this structure offers enhanced adaptability. Certain patches can be strategically heated to high temperatures to increase damping, while others remain at low temperatures to preserve stiffness [6, 23]. This approach enables the structure to be programmed for optimal performance under diverse operating conditions.

Thanks to its reduced computational time, the equivalent plate model is used to explore the various behaviors of this heterogeneous sandwich plate. Each patch is represented by a set of effective properties that depend on both frequency and temperature. A total of 1,024 thermal configurations (*i.e.*, the arrangement of patches and temperatures) are randomly generated, and the vibroacoustic indicators of the samples are evaluated. The configuration shown in Figure 10 was selected from this set to achieve a balance between vibration reduction across the entire frequency range and maintaining structural stiffness. Temperatures are indicated at the center of each patch.

The finite element implementation of the equivalent plate allows for the consideration of any type of boundary conditions and spatially varying mechanical properties across the plate's surface (along its length and width). In this study, temperature gradients between patches are neglected. However, interfaces between patches - treated as distinct zones at averaged temperatures - can still be accounted for in the plate modeling.

The left edge of the heterogeneous plate in Figure 10 is clamped ($x = 0$ mm), while the remaining edges are free (cantilever boundary condition). A harmonic point load with unit amplitude is applied at $x_0 = 375.0$ mm and $y_0 = 262.5$ mm. As in the previous cases, the high-fidelity model is constructed using TET10 solid elements, with one finite element per layer in the transverse direction of the sandwich plate. For the heterogeneous sandwich plate case, an equal number of finite elements is assigned to each patch. Convergence was assessed based on the mean square velocity. The equivalent plate model is again constructed using DKTP elements, ensuring that each patch contains the

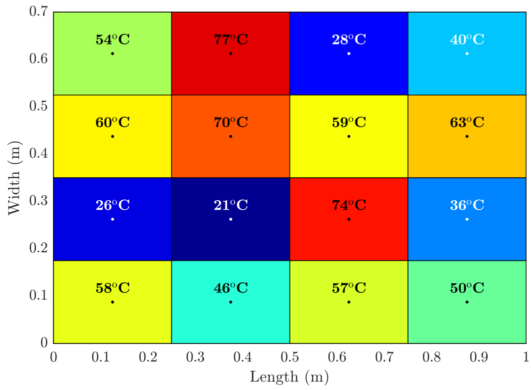

Figure 10: Equivalent plate divided into patches: the thermal configuration contains high damping patches.

same number of elements. A convergence study was also conducted based on the mean square velocity. Figure 11 presents the mean square velocity and the driving-point mobility for this thermal configuration.

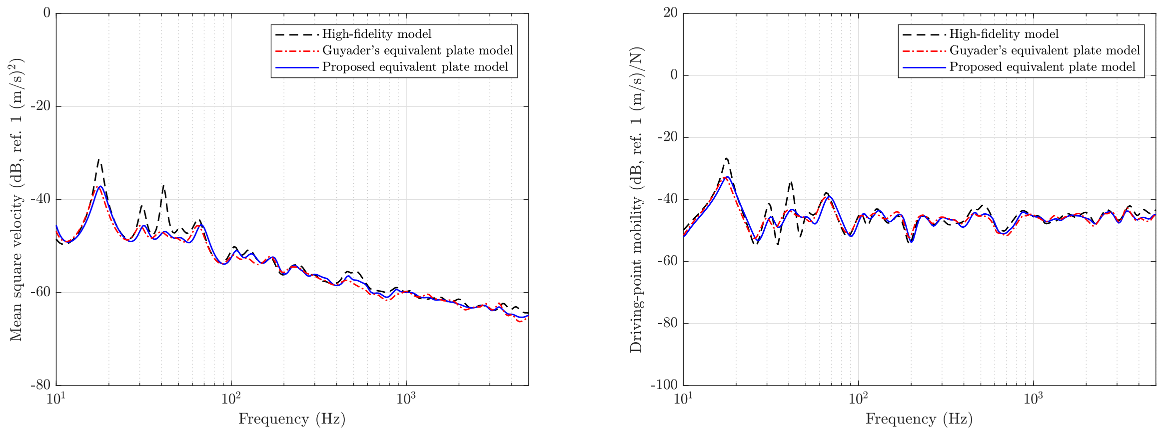

Figure 11: Mean square velocity and driving-point mobility of the heterogeneous sandwich plate clamped at one edge and free at the others (C-F-F-F): high-fidelity model (408,875 nodes); proposed equivalent plate model (5,785 nodes).

Overall, the equivalent plate model can assess the behavior of the structure when high damping patches are considered. To emphasize the efficiency of the proposed equivalent plate model, results are achieved in less than two minutes, compared to seven hours for the high-fidelity finite element model of the sandwich plate.

3.3. Damping loss factor estimation using the proposed equivalent plate FE model

The equivalent plate finite element models - constructed using the effective bending stiffness and damping loss factor obtained from both Guyader's model and the proposed model (Figures 4, 5 and 6) - are then used to estimate structural damping based on the Power Input Method (Equation 21). The effectiveness of the proposed model is demonstrated in Figure 12.

Clearly, the equivalent plate adopting the equivalent damping definition $\eta = \frac{\Im(\tilde{D})}{\Re(\tilde{D})}$ - as used in Guyader's model (and other models such as the RKU model - is not suitable for estimating the high structural damping levels. In contrast, the proposed model provides estimates that more closely match the high-fidelity reference model. To illustrate

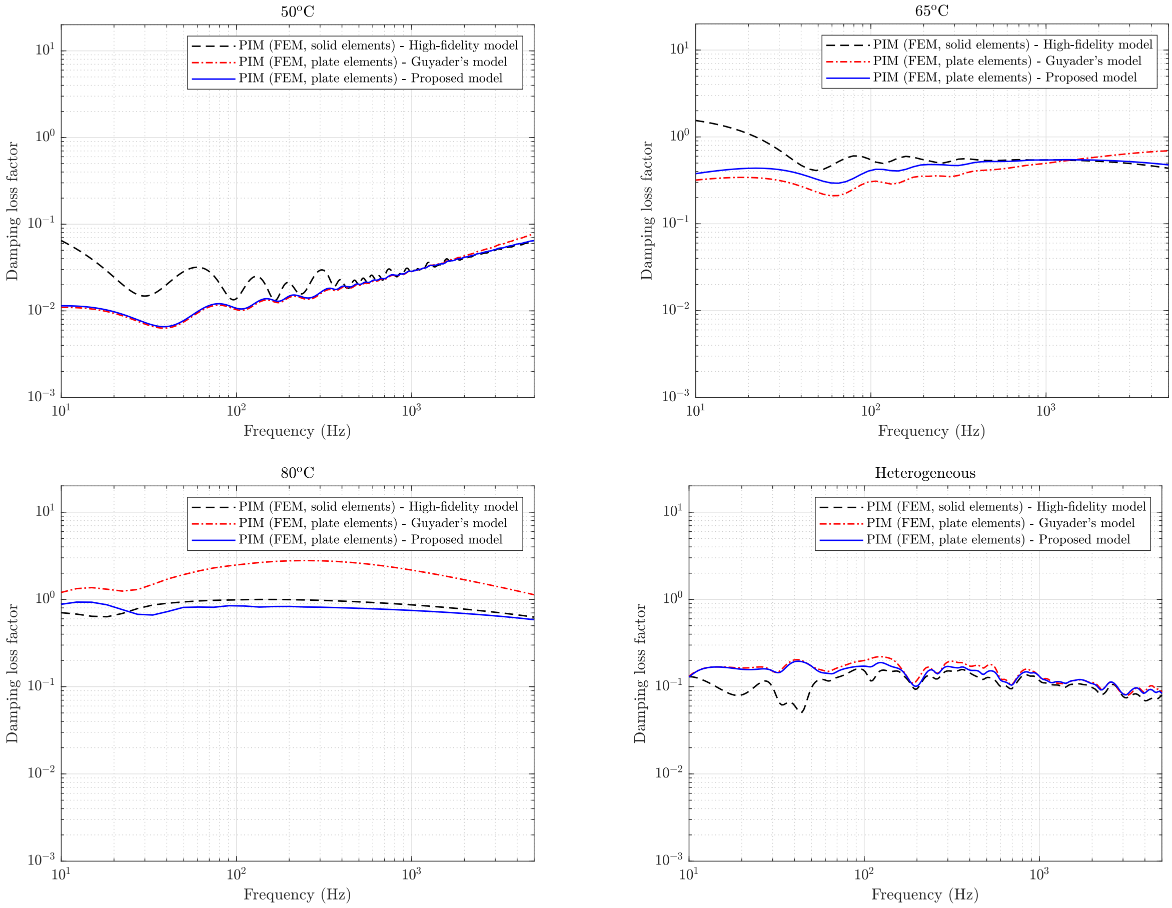

Figure 12: Comparison of structural damping estimates obtained using the Power Input Method and the equivalent plates defined by Guyader's model and the proposed model.

this, the average damping loss factor $\bar{\eta}$ is calculated by solving Equation 25:

$$\bar{\eta} = \frac{1}{\omega_2 - \omega_1} \int_{\omega_1}^{\omega_2} \eta(\omega)\, d\omega, \tag{25}$$

where $\eta(\omega)$ is obtained using Equation 21, and the interval $[\omega_1, \omega_2]$ covers the entire frequency range. Table 4 presents the relative error in the average structural damping loss factor.

Case	Average Damping Loss Factor (Equation 25)			Relative error (%)	
	high-fidelity	Guyader's	Proposed	Guyader's	Proposed
50°C	0.044	0.048	0.044	9	0
65°C	0.505	0.584	0.513	16	2
80°C	0.765	1.686	0.681	120	11
Heterogeneous	0.095	0.111	0.108	18	14

Table 4: Comparison of structural damping loss factor estimates using different equivalent plate models and their relative errors with respect to a high-fidelity sandwich plate model. The proposed equivalent plate model shows significantly lower relative error compared to Guyader's model, demonstrating improved accuracy on damping estimation.

For the proposed equivalent plate, the loss factor is determined using the power balance equation and the GLM forced response. In contrast, the equivalent plate based on Guyader's properties adopts an equivalent (simplified) damping definition. The results show that the proposed equivalent plate consistently outperforms Guyader's model in all damping estimation cases, notably when high damping levels are involved.

4. Conclusion

This paper describes a methodology for modeling highly damped sandwich plates using an equivalent single-layer thin plate representation. The effective properties of the equivalent plate are explicitly calculated by preserving the real part of bending, shear (transverse) and extension (quasi-longitudinal) wavenumbers. These variables are estimated using a semi-analytic discrete model to compute the dispersion relations in multilayered plates. Structural damping loss factor is considered, and the damping estimate is based on the power balance equation, accounting for the contribution of various waves types through the computation of the forced response of the sandwich plate in the wave domain. The present damping estimate is accurate, compared to the damping values obtained through the Power Input Method using the full order finite element model of the sandwich plate. This approach is suitable for highly damped configurations, where other damping formulations fail to provide accurate estimates. Furthermore, the computational time to estimate damping is reasonable, requiring only a few seconds. The effective properties are used in the definition of a finite element model of the equivalent plate, and the key points of this study are as follows:

- The proposed equivalent plate model accurately describes the behavior of sandwich plates with low to moderate damping levels, matching the vibroacoustic indicators of the full order model while significantly reducing the number of degrees of freedom;
- Despite some deviations for high damping levels cases (55% and 77%), the equivalent plate model accurately captures the overall trends in the vibration response of the sandwich plate;
- Compared to other models, the proposed equivalent plate model is more accurate in estimating the damping of the sandwich structure using the power balance equation, due to the adopted damping definition;
- The finite element implementation of the proposed equivalent plate model is suitable for assessing the behavior of the sandwich plate assuming various boundary conditions, homogeneous and heterogeneous temperature fields (*i.e.,* contrasted properties) along the viscoelastic core.

The proposed equivalent plate model demonstrates a substantial reduction in computational time, making it a practical tool for understanding the behavior of sandwich plates in the early design stage. In addition, the methodology can be adopted for multilayered plates in general (sandwich plates with symmetric or asymmetric configurations with soft core, arbitrary number of layers). Depending on the required accuracy, the proposed model can be used for applications requiring iterative analyses, such as optimization and parameter estimation problems, propagating of uncertainties, etc.

Future studies should focus on the experimental validation of the effective properties and damping estimates. In the context of a real-time vibration control application, an adaptive sandwich plate can be divided into patches assuming different temperatures, and the model can be used to determine optimal thermal configurations for a compromise between damping and stiffness.

CRediT authorship contribution statement

Rafael da S. Raqueti: Conceptualization, Methodology, Investigation, Writing - original draft, Writing - review and editing. **Noureddine Atalla:** Conceptualization, Methodology, Resources, Supervision, Writing - review and editing. **Morvan Ouisse:** Conceptualization, Methodology, Resources, Supervision, Writing - review and editing. **Emeline Sadoulet-Reboul:** Conceptualization, Methodology, Resources, Supervision, Writing - review and editing.

Declaration of competing interest

The authors declare that they have no known competing financial interests or personal relationships that could have appeared to influence the work reported in this paper.

Data availability

Data will be made available on request.

Acknowledgements

The authors would like to thank the Natural Sciences and Engineering Research Council of Canada (NSERC); ISITE-BFC (ANR-15-IDEX-0003); and EUR EIPHI (ANR-17-EURE-0002) for their financial support.

Appendix A. Analytical solution using a modal approach

Assuming a transverse harmonic point load of magnitude F is applied at the coordinates (x_0, y_0), the transverse velocities of the sandwich plate can be analytically determined, as formulated in Equation A.1:

$$\frac{v(x,y)}{F} = \sum_{m=1}^{\infty}\sum_{n=1}^{\infty} \frac{\phi_{mn}(x_0, y_0)}{N_{mn}\, Z_{mn}} \phi_{mn}(x,y), \tag{A.1}$$

where $\phi_{mn}(x,y)$ is the mode shape, N_{mn} the mode norm, and Z_{mn} is the modal impedance. These variables depend on the boundary conditions of the sandwich plate. Generalizing for various boundary conditions:

$$\phi_{mn}(x,y) = \varphi_m(x)\,\varphi_n(y), \tag{A.2}$$

$$N_{mn} = \int_0^{L_x}\int_0^{L_y} \phi_{mn}^2(x,y)\; dy\, dx. \tag{A.3}$$

The modal impedance Z_{mn} can also be determined by using the GLM formulation. The wavenumbers pair $(k_m, k_n) = \left(\frac{\lambda_m}{L_x}, \frac{\lambda_n}{L_y}\right)$ are defined, with λ_i, $i = m, n$ a parameter depending on the boundary conditions, and $k_{mn} = \sqrt{k_m^2 + k_n^2}$. Equation A.4 gives the modal mixed displacement-force vector response $\{\mathbf{e}_{mn}\}$:

$$\{\mathbf{e}_{mn}\} = \left(k_{mn}^2\left[\mathbf{A}_2(\varphi)\right] - jk_{mn}\left[\mathbf{A}_1(\varphi)\right] - \left[\mathbf{A}_{01}(\varphi)\right] - \omega^2\left[\mathbf{A}_{02}(\varphi)\right]\right)^{-1}\{\mathbf{F}\}. \tag{A.4}$$

By selecting the loading degree of freedom from the response, $v_{mn} = j\omega\{e_{mn}\}$. Finally, the modal impedance is:

$$Z_{mn} = \frac{1}{v_{mn}}. \tag{A.5}$$

For a simply supported sandwich plate, $\lambda_i = i\pi$, with $i = m, n$, $N_{mn} = \frac{L_x L_y}{4}$, and $\phi_{mn}(x,y) = \sin(k_m x)\sin(k_n y)$. Solutions for other boundary conditions are available in the references [31, 32]. This approach can be used to evaluate the vibroacoustic indicators, such as the mean square velocity of the sandwich plate with a homogeneous temperature field on the core.

References

[1] A. M. Baz, Active and Passive Vibration Damping, Wiley, 2018. doi:10.1002/9781118537619.

[2] Y. Liu, L. Wang, Y. Liu, F. Zhang, J. Leng, Recent progress in shape memory polymer composites: Driving modes, forming technologies, and applications, Composites Communications 51 (2024) 102062. doi:10.1016/j.coco.2024.102062.

[3] P. Butaud, M. Ouisse, V. Placet, F. Renaud, T. Travaillot, A. Maynadier, G. Chevallier, F. Amiot, P. Delobelle, E. Foltête, C. Rogueda-Berriet, Identification of the viscoelastic properties of the tBA/PEGDMA polymer from multi-loading modes conducted over a wide frequency–temperature scale range, Polymer Testing 69 (2018) 250–258. doi:10.1016/j.polymertesting.2018.05.030.

[4] P. Butaud, E. Foltête, M. Ouisse, Sandwich structures with tunable damping properties: On the use of Shape Memory Polymer as viscoelastic core, Composite Structures 153 (2016) 401–408. doi:https://doi.org/10.1016/j.compstruct.2016.06.040.

[5] M. Ouisse, D. Renault, P. Butaud, E. Sadoulet-Reboul, Damping control for improvement of acoustic black hole effect, Journal of Sound and Vibration 454 (2019) 63–72. doi:10.1016/j.jsv.2019.04.029.

[6] P. Butaud, D. Renault, B. Verdin, M. Ouisse, G. Chevallier, In-core heat distribution control for adaptive damping and stiffness tuning of composite structures, Smart Materials and Structures 29 (6) (2020) 065002. doi:10.1088/1361-665x/ab802a.

[7] D. A. Rade, J.-F. Deü, D. A. Castello, A. M. G. de Lima, L. Rouleau, Passive Vibration Control Using Viscoelastic Materials, Springer International Publishing, 2019, pp. 119–168. doi:10.1007/978-3-030-13317-7_5.
[8] E. Carrera, Theories and Finite Elements for Multilayered, Anisotropic, Composite Plates and Shells, Archives of Computational Methods in Engineering 9 (2) (2002) 87–140. doi:10.1007/bf02736649.
[9] E. Carrera, Theories and Finite Elements for Multilayered Plates and Shells: A Unified compact formulation with numerical assessment and benchmarking, Archives of Computational Methods in Engineering 10 (3) (2003) 215–296. doi:10.1007/bf02736224.
[10] S. Ghinet, N. Atalla, Modeling thick composite laminate and sandwich structures with linear viscoelastic damping, Computers & Structures 89 (15) (2011) 1547–1561. doi:https://doi.org/10.1016/j.compstruc.2010.09.008.
[11] P. J. Shorter, Wave propagation and damping in linear viscoelastic laminates, The Journal of the Acoustical Society of America 115 (5) (2004) 1917–1925. doi:10.1121/1.1689342.
[12] E. Manconi, B. R. Mace, Estimation of the loss factor of viscoelastic laminated panels from finite element analysis, Journal of Sound and Vibration 329 (19) (2010) 3928–3939. doi:10.1016/j.jsv.2010.04.014.
[13] C. Boutin, K. Viverge, Generalized plate model for highly contrasted laminates, European Journal of Mechanics - A/Solids 55 (2016) 149–166. doi:10.1016/j.euromechsol.2015.08.008.
[14] C. Boutin, K. Viverge, S. Hans, Dynamics of contrasted stratified elastic and viscoelastic plates - application to laminated glass, Composites Part B: Engineering 212 (2021) 108551. doi:10.1016/j.compositesb.2020.108551.
[15] D. Ross, E. Ungar, E. J. Kerwin, Damping of plate flexural vibrations by means of viscoelastic laminae, Structural damping 6 (6) (1959) 49–97. doi:10.12691/jmdv-5-1-3E.
[16] J. L. Guyader, C. Lesueur, Acoustic transmission through orthotropic multilayered plates, part I: Plate vibration modes, Journal of Sound and Vibration 58 (1) (1978) 51–68. doi:10.1016/s0022-460x(78)80060-1.
[17] J.-L. Guyader, C. Cacciolati, Viscoelastic properties of single layer plate material equivalent to multi-layer composites plate, in: INTER-NOISE and NOISE-CON Congress and Conference Proceedings, Vol. 2007, Institute of Noise Control Engineering, 2007, pp. 4190–4199.
[18] U. Arasan, F. Marchetti, F. Chevillotte, L. Jaouen, D. Chronopoulos, E. Gourdon, A simple equivalent plate model for dynamic bending stiffness of three-layer sandwich panels with shearing core, Journal of Sound and Vibration 500 (2021) 116025. doi:10.1016/j.jsv.2021.116025.
[19] K. Ege, N. B. Roozen, Q. Leclère, R. G. Rinaldi, Assessment of the apparent bending stiffness and damping of multilayer plates; modelling and experiment, Journal of Sound and Vibration 426 (2018) 129–149. doi:10.1016/j.jsv.2018.04.013.
[20] F. Marchetti, K. Ege, Q. Leclère, N. Roozen, On the structural dynamics of laminated composite plates and sandwich structures; a new perspective on damping identification, Journal of Sound and Vibration 474 (2020) 115256. doi:10.1016/j.jsv.2020.115256.
[21] D. Cui, N. Atalla, M. Ichchou, A.-M. Zine, Damping prediction of highly dissipative meta-structures through a wave finite element methodology, Mechanical Systems and Signal Processing 215 (2024) 111408. doi:10.1016/j.ymssp.2024.111408.
[22] D. M. Tuozzo, N. Atalla, Multi-wave-based semi-analytical homogenization approaches for the vibroacoustics of elastic multilayered structures including curvature, orthotropy, asymmetry, high shear and high damping, Mechanical Systems and Signal Processing 225 (2025) 112248. doi:10.1016/j.ymssp.2024.112248.
[23] P. Butaud, M. Ouisse, G. Chevallier, E. Foltête, Design of thermally adaptive composite structures for damping and stiffness control, in: Behavior and Mechanics of Multifunctional Materials and Composites 2017, Vol. 10165, Portland, Oregon, United States, 2017, p. 101650T. doi:https://doi.org/10.1117/12.2259873.
[24] M. Collet, M. Ouisse, M. Ruzzene, M. Ichchou, Floquet–bloch decomposition for the computation of dispersion of two-dimensional periodic, damped mechanical systems, International Journal of Solids and Structures 48 (20) (2011) 2837–2848. doi:https://doi.org/10.1016/j.ijsolstr.2011.06.002.
[25] K. Billon, M. Ouisse, E. Sadoulet-Reboul, M. Collet, P. Butaud, G. Chevallier, A. Khelif, Design and experimental validation of a temperature-driven adaptive phononic crystal slab, Smart Materials and Structures 28 (3) (2019) 035007. doi:10.1088/1361-665X/aaf670.
[26] R. Cherif, N. Atalla, Experimental investigation of the accuracy of a vibroacoustic model for sandwich-composite panels, The Journal of the Acoustical Society of America 137 (3) (2015) 1541–1550. doi:10.1121/1.4908239.
[27] D. Bies, S. Hamid, In situ determination of loss and coupling loss factors by the power injection method, Journal of Sound and Vibration 70 (2) (1980) 187–204. doi:10.1016/0022-460x(80)90595-7.
[28] M. N. Bin Fazail, J.-D. Chazot, G. Lefebvre, N. Atalla, Damping loss factor characterization of complex structures using a green's function-based model, Journal of Sound and Vibration 552 (2023) 117642. doi:10.1016/j.jsv.2023.117642.
[29] V. Gerasik, M. Stastna, Complex group velocity and energy transport in absorbing media, Physical Review E 81 (5) (2010) 056602. doi:10.1103/physreve.81.056602.
[30] J.-L. Batoz, G. Dhatt, Modélisation des structures par éléments finis, Presses Université Laval, 1990.
[31] J. N. Reddy, Mechanics of Laminated Composite Plates and Shells, Taylor & Francis Ltd., 2003.
[32] J. M. Berthelot, J. M. Cole, Composite Materials: Mechanical Behavior and Structural Analysis, Mechanical Engineering Series, Springer New York, 2012.